Scientific Research Publishing

Journal of Biosciences and Medicines, 2024, 12, 38-54
https://www.scirp.org/journal/jbm
ISSN Online: 2327-509X
ISSN Print: 2327-5081

Validation of the TOPAS Monte-Carlo Code of the Off-Field Dose of a 6 MV Synergy Linac

Kodjo Joel Fabrice N'Guessan[1,2*], Ibrahima Sakho[1], Bogbé D. L. H. Gogon[3]

[1]Department of Physics and Chemistry, Faculty of Sciences and Technology, Iba Der Thiam University of Thiès, Thiès, Senegal
[2]International Cancer Center of Dakar, Dakar, Senegal
[3]Department of Physics, Faculty of Sciences and Technology, Félix Houphouet Boigny University of Abidjan, Abidjan, Côte d'Ivoire
Email: *joelfabrice.nguessan@gmail.com

How to cite this paper: N'Guessan, K.J.F., Sakho, I. and Gogon, B.D.L.H. (2024) Validation of the TOPAS Monte-Carlo Code of the Off-Field Dose of a 6 MV Synergy Linac. *Journal of Biosciences and Medicines*, **12**, 38-54.
https://doi.org/10.4236/jbm.2024.127005

Received: June 3, 2024
Accepted: July 6, 2024
Published: July 9, 2024

Abstract

The risk of radiation-induced second cancer and the late tissue loss due to Off-field doses in radiotherapy remain a serious concern. Monte Carlo (MC) simulation is currently one of the most accurate methods for calculating these doses. MC simulation model based on the Particle Simulation Tool (TOPAS) has been developed to simulate the off-field dose of an Elekta Synergy linear accelerator (Linac) emitting 6 MV photons. Measurements were taken in a water phantom using an ionization chamber to validate this model. The Percentage Depth Dose (PDD) at the depth of 0.0, 5.0, 10.0 and 15.0 cm from the beam axis for a 10 × 10 cm^2 field size was measured and simulated. Off-field dose profiles at the depth of 1.5 (d_{max}), 5.0 and 10.0 cm for field sizes of 5 × 5, 10 × 10, 15 × 15, and 20 × 20 cm^2 respectively were measured and simulated. Comparison of measured and simulated off-field dose values showed a good agreement. The average gamma passing rate of the PDDs and profiles curves for off-field doses were 87.5% and 98.11% respectively. The local dose difference based on the PDD curve between the measured and simulated was less than 6.0 % for all locations. For all field size considered in this study, the average difference between profile curves for off-field dose measured and simulated was 9.1%. PDDs and Profiles curves for off-field dose simulation uncertainties were less than 2.0% and 1.0% respectively. TOPAS-MC simulation model developed is a good representation of our 6 MV Linac Elekta Synergy for assessing off-field dose, which would be the primary cause of some secondary cancers.

Keywords

Radiotherapy, Off-Field Dose, Secondary Cancer, TOPAS-MC Simulation,

Dosimetry

1. Introduction

External beam radiotherapy (EBRT) involves a high-energy ionizing radiation, depending on the tumor and organ types, which passes through the skin and healthy tissue to destroy the tumor while sparing the surrounding healthy tissue. However, during the treatment, healthy tissue can be close or far from the tumor or outside the treatment field that could receive low or high doses. These low doses often are poorly considered in treatment planning and evaluation, it is therefore necessary to develop tools to assess the average dose for various organs at risk of the patient during the treatment course. Thus, these low dose levels have been relatively associated with radiation-induced cancer in patients after the course of the treatment. Several studies have shown that these low doses could induce late effects including cardiovascular disease, respiratory and digestive diseases [1], cataracts [2], as well as the induction of secondary cancer in patients after radiotherapy [3] [4]. In addition to that, off-field radiation is also one of particular interest in the treatment of pregnant patients, because these peripheral low doses of 5cGy, is particularly harmful to the fetus [5]. The challenge is to achieve the optimum treatment by balancing the risk and the benefit [5]. The quantification of low doses due to off-field dose in radiotherapy would improve the understanding of secondary radiation-induced cancer and assist in the development of strategies to reduce these exposures. In RT, the off-field dose measurement requires a suitable or specific phantom based on the tedious placement of various calibrated dosimeters in each corresponding cavity for each specific case. However, these measurements are extremely time-consuming. To overcome these challenges, computational techniques such as Monte Carlo (MC) models are an alternative to the off-field dose measurements.

The MC model is one of the most accurate simulation methods for calculating dose distributions, particularly inside homogeneous phantom where the effects of electron transport cannot be accurately calculated by conventional methods using deterministic algorithms [6]. With this model, the modelling of the head of the Linac used in RT provides several parameters such as the fluence and mean energy distributions. This study was carried out to validate a new MC model for off-field dose calculated using an appropriate Tool for Particle Simulation Monte Carlo (TOPAS-MC) code for different field sizes at different depths. To this end, we compared the measured and simulated off-field dose at different distances from the field axis, and at different depths using the Elekta Synergy with 6 MV photon beams. The relative dose difference and gamma index approach [7] were used to evaluate and analyze measured and simulated off-field dose values.

2. Materials and Methods

2.1. Accelerator Geometry

Technical drawings of Linac head components and material data (densities and mixtures) for a 6 MV photon beam have been supplied by Elekta manufacturer under a confidentiality agreement. For these reasons, certain components are not shown in details including their actual sizes or positions. The components simulated are represented in Figure 1 as follows:

- Elements that are highly dependent on the selected irradiation energy, namely the X-ray target and the flattening filter;
- Invariant elements such as the primary collimator, ionization chamber and mirror;
- Other elements that depend on beam shape such as multi-leaf collimators (MLCs) and asymmetrical Y jaws.

The coordinates of the treatment head are expressed in a Cartesian coordinate system. Hence, the (Oz) axis corresponds to the radiation axis, with the origin located on the upper face of the X-ray target. All details are represented in Figure 1 below.

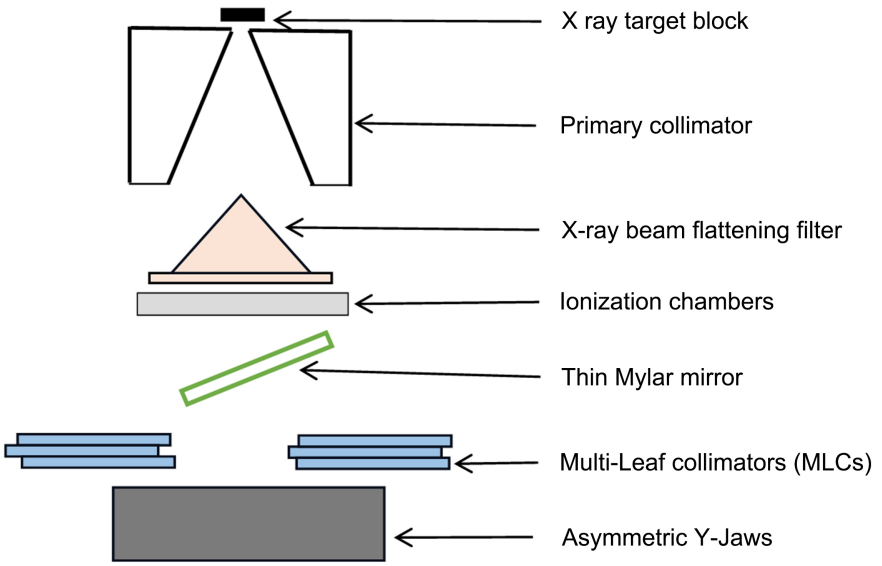

Figure 1. Component of Elekta Synergy Linac head for 6 MV Beam, include X-ray, primary collimator, flattening filter, ionization chamber, mirror, multi-leaf collimators and asymmetric Y-jaws.

2.2. Experimental Measurements

Linac Elekta Synergy with 6 MV photon beams used clinically are considered as a no neutron producing beam. Matsubara *et al.* have recently reported that only few neutrons are produced from a 6-MV beam [8]. Measurements were carried out using a PTW motorized water phantom (ScanLift) builds with a plexiglass. Inner dimensions of the water phantom were 60 cm × 60 cm × 50 cm, fitted with a high-precision 3D motion mechanism made of stainless steel. It has three

stepper motors for detector positioning with a speed of 50 mm/s, and a positioning accuracy of ±1 mm. The phantom tank is equipped with a TBA CONTROL PENDANT (T41031) hand-held controller for connection to an ionization chamber adjuster, a TBA CONTROL UNIT (T41013) controller and a TANDEM dual-channel electrometer for dose distribution and beam analysis in radiotherapy. The device was controlled by MEDPHYSTO software (Version 3.4.1). Prior to the measurement, the Linac was calibrated according to IAEA protocol TRS-398 in a water phantom [9]. Dose distributions were measured in a 60 × 60 × 50 cm^3 water phantom in-plane direction, and at a source-to-surface distance (SSD) of 100 cm for all field sizes used. Percentage Depth Dose (PDD) was measured using a 0.3 cm^3 PTW Semiflex ionization chamber (TM31013) on the surface of the water phantom, at a depth of 25.0 cm in water. PDD measurements were taken at depth of 0 cm, 5 cm, 10 cm, and 15 cm from the central axis, and were normalized to the dose maximum (d_{max}). In addition to that, the dose profile was measured for field sizes of 5 × 5 cm^2, 10 × 10 cm^2, 15 × 15 cm^2, and 20 × 20 cm^2 using a PTW microdiamond chamber (TM60019). For each field size, the chamber was placed at the depth of 1.5 cm, 5.0 cm and 10.0 cm in the water phantom respectively. All dose profiles were normalized to the percentage of central axis (% of CAX).

2.3. Simulation Parameters

2.3.1. TOPAS Monte Carlo Model

The TOPAS code (Tool for Particle Simulation) version 3.9 [10] was used to simulate particle interactions in a water phantom. This tool is a C++ application that wraps and extends the Geant 4 simulation toolbox, version 10.5.p01 [11]. It has been developed in order to make Monte Carlo simulations user-friendly in the fields of physics, biology and clinical research. TOPAS-MC uses the Monte Carlo method to simulate the transport of radiation through any complex geometry, including medical instruments, detectors and patients. It models any fundamental particle such as photons, electrons, protons and heavy ions, and allows to import the patients through DICOM images, and other image formats [10]. TOPAS-MC developers have integrated a platform for the four-dimensional simulation of all forms of radiotherapy [12]. They have also allowed to manage complex movements through its system of temporal characteristics, while taking into account the temporal dependencies of modern therapies such as particle beams, Linac head components, and patient movements (breathing, heartbeat, etc.) [13]. The main advantage of TOPAS is based on its parameter control system that lets you assemble and control a rich library of simulation objects (geometry components, particle sources, scorers, etc.) with no need to write C++ code. Advanced users remain free to implement their own simulation objects in C++ code, and add them to TOPAS via an extension mechanism [11] [12]. The control system is described in the first general TOPAS-MC document [10] [14]. Simulation of the transport of photons, electrons and positrons

through the Linac head has been carried out considering the following interaction processes: Compton Scattering, Gamma Conversion, Photoelectric Effect for Photons, Multiple Scattering, Ionization and Bremsstrahlung for Electrons and Positrons. The TOPAS-MC code provides several physics modules, including the g4em-standart_opt4 model that was used in this work as it was developed specifically to model the transport of photons and charged particles for radiotherapy purposes. As disadvantage, the TOPAS MC does not contain explicit instructions about building or running process from initial stage, but it only determines what to do at run time according to a set of user-supplied text files called TOPAS Parameter Control.

2.3.2. Variance Reduction Technique

Despite simulation times of up to several weeks, the uncertainty associated with the calculated variable may still be too high for the user's needs. Various techniques can be used to reduce the variance [12] [15]. The latter must be adapted to the problem type being modeled. In some cases, they may be more costly in terms of computing time per primary simulated particle than an analogous simulation [15]. Most of particles that reach the phantom are bremsstrahlung gamma, the selective bremsstrahlung splitting. The variance reduction technique used in this study is bremsstrahlung Splitting, which is closely related to the purpose of the simulation, which is to simulate a larger number of stories while reducing calculation time and obtaining better precision. This bremsstrahlung splitting was performed with the energy threshold > 6.7 MeV to enable the split.

Indeed, given that the simulation is used to evaluate the dose distribution in a phantom or patient, it is interesting to have a large number of photons, which will increase statistical precision by reducing the variance. In this technique, the photon generated in the bremsstrahlung process due to the interaction of the electron with the gas pedal target is generated N times, and the weight of each photon will be 1/N. All photons are created with the same probability, irrespective of their energy and direction [15]. In the Topas-MC code, certain criteria including Secondary Biased approach can be used to increase the efficiency of the bremsstrahlung splitting technique.

In this case, variance reduction works with electromagnetic physical process and region. The physical regions allow several components to have specific production cuts. This is useful in complex geometrical configurations to improve calculation speed by assigning high production cuts in regions where detailed simulation is not important. Three vectors are then defined: one with the name of the electromagnetic processes, another one with the division number for each process, and finally with the maximum energies for each process. Biased particles with energies above these values are subjected to Russian roulette [10].

2.3.3. Linac Head Simulation

The Linac coordinates described in TOPAS-MC are as follows: the positive z-axis spans from the iso-center to the target (beam-line direction), the positive

x-axis from the iso-center to the right of the patient lying on the treatment table (cross-plane direction), and the positive y-axis from the iso-center to the head of the patient lying on the table (in-plane direction). In our simulation, each component of the Linac head was described in terms of shape, size, position, material composition and density. The electron and photon cut-off distances were set at 0.1 mm. The cut-off distance is the distance at which the particles are no longer tracked, or at which the MC simulation stops particle transport if the particle falls below this value [16]. The simulation process was carried out in two stages: The first step was to create the phase space by simulating the independent part of the patient from the target to the mirror (**Figure 2**). The phase space file contains information on particle type, direction, three-dimensional (3D) coordinates, production process, weight and energy of incoming particles located before the MLCs [17]. Results of the phase-space file, containing 8×10^8 particles positioned at 72.79 cm from the iso-center, just before the MLCs, and used as a photon source. The components simulated can be summarized as follows:

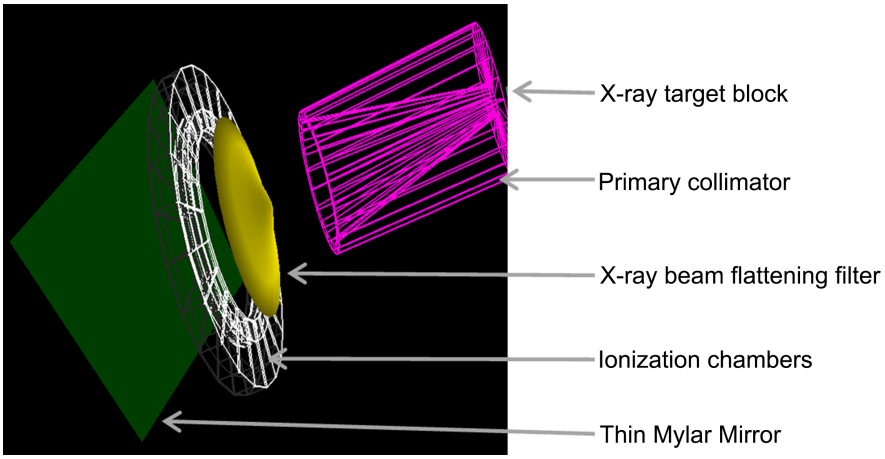

Figure 2. Simulation of patient-independent Linac head components with TOPAS-MC.

- X-ray target: generates bremsstrahlung X-rays using a thin tungsten and rhenium disk with a radius of 2.7 mm and a thickness of roughly 0.89 mm. The remaining primary electrons are absorbed in a copper absorber disk with a thickness of approximately 10 mm and a radius of 10 mm;
- Primary collimator: it was made of tungsten alloy, about 101 mm in height. located at 67.15 mm just below the target. This component was used for two reasons, the first was to collimate the photons in the direction of the treatment field; and the other was to reduce the leakage radiation outside the field area;
- Xray beam flattening filter: made of a mixture of manganese, chromium, carbon, iron, phosphor, and nickel, about 32.05 mm in height including the cylindrical base, located at 141.5 mm just below the primary collimator. A precisely specified surface configuration is attached (combining cones with various radiuses) to the lower end of the primary collimator and gives regular

radiation intensity distribution across fields;

- Ionizing chambers: made of polarizing mylar films, aluminum and ceramic motherboards, separated by spacers made of air, located at 170 mm just below the flattening filter. Designated for beam monitoring of photon and electron radiation production;
- Mylar mirror: constructed of a thin mylar material. This segment is located at 225.1 mm under the dose ionizing chambers on the beam focal axis to facilitate patient setup and show the location and shape of the radiation beam.

For our simulation, the electron beam on the target was characterized by an average energy of 6.7 MeV. The Full Width Half Maximum (FWHM) of the electron beam Gaussian energy distribution was kept constant at 3% of the mean energy, and a spot size was 1mm FWHM. The patient-independent Linac head components with TOPAS-MC are represented in **Figure 2**.

The second step was to simulate the Y-jaws, the MLCs, and to measure the relative dose in a water phantom under the same conditions as the experimental measurements. Thus, PDD curves and dose profiles were simulated. The components simulated can be summarized as follows:

- multi-leaf collimator MLC: made of tungsten alloy, about 90 mm in thickness and 155 mm in height, located just below the Phase Space position (280 mm), used for precise treatment and the most accurate conformal beam shaping for treatments;
- secondary collimators Y: is made of tungsten alloy and have about 77 mm of thickness. They are used to minimize the inter-leaf leakage and set the treatment field's overall size.

Finally, average doses were calculated to obtain the best balance between calculation times and uncertainties in low-dose regions. In order to achieve good agreement between measurement and simulation, and to reduce the statistical uncertainty of the calculated dose [18], the tuning and the validation process for Linac models were introduced using the voxel size of 1.0 cm × 1.0 cm × 1.0 cm for all simulations. Studies have shown that a large voxel size is necessary to simulate doses out of range to achieve reasonable statistical results. As these areas have extremely small doses, this may lead to uncertainty The large size of the voxel helps to reduce the statistical uncertainty of the calculated dose in every voxel [16] [18]. **Figure 3** shows the Multi-Leaf Collimators (**Figure 3(a)**), and an asymmetrical Y Jaws (**Figure 3(b)**) simulated, and **Figure 4** illustrates the dose calculation stage. For each simulation, the statistical uncertainty has been calculated accordingly [19]. All details are represented in **Figure 3** and **Figure 4** that are found in supplementary material.

In this study, the pre-defined acceptance criteria are based on the dose difference and distance-to-agreement. PDDs and dose profiles were analyzed with 3% and 3 mm. These criteria were selected to increase the efficiency of the output results statistically on the one hand. On the other hand, the global gamma index analysis was used for validation of gamma passing rate.

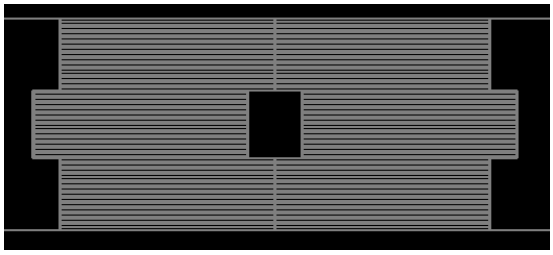

(a)

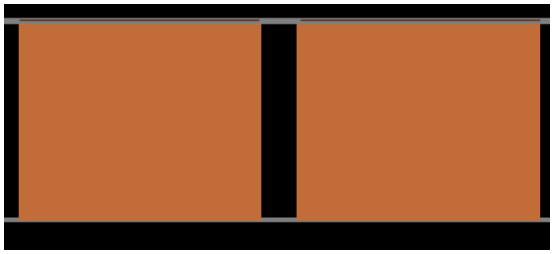

(b)

Figure 3. Simulation of the Multi-Leaf Collimators (a), and an asymmetrical Y Jaws (b) with TOPAS-MC.

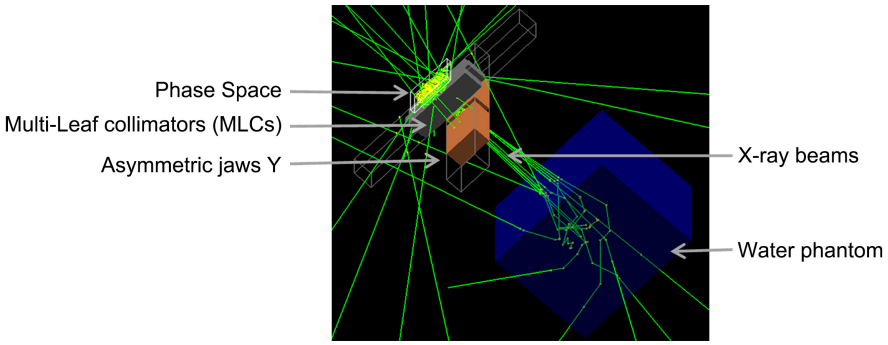

Figure 4. Dose calculation stage in Monte Carlo simulation showing phase space source, MLCs, X-rays beam (green lines), and water phantom with TOPAS-MC.

3. Results

The results of the in-field and off-field validation of the 6 MV Elekta Synergy accelerator model, were summarized in Table 1 and Table 2 respectively. Figure 5 shows the comparison between the measure and simulate PDD curves in-field and off-field, for 6 MV beam along the in-plane direction at 0.0, 5.0 and 10.0 and 15.0 cm respectively from the beam axis, with the field size 10 × 10 cm^2. The simulated d_{max} for the 10 × 10 cm^2 field size was 1.6 cm compared to a measure value of 1.5 cm.

Table 1 shows the relative dose difference and gamma passing rate between the measured and simulated in-field and off-field PDD, as well as statistical uncertainty of simulation. The comparisons between the PDD measured and simulated in-field (Figure 5(a)), and penumbra (Figure 5(b)) shows the best agreement in terms of gamma index compared to off-field PDD. Figure 5(c) and Figure 5(d) for off-field PDD curves at 10.0 cm and 15.0 cm from axis show

similar result of measured and simulated curves, with a noisy appearance for simulated PDD. The acceptance criteria for gamma index analysis were 3% 3 mm. The results are shown in the Table 1 and Figure 5 respectively.

Table 1. The relative dose difference and gamma-index values between the measured and simulated in-field and off-field PDD curves, and statistical uncertainty of simulation.

Distance from central axis (cm)	Relative Difference (%)	Gamma passing rate (%)	Uncertainty (%)
0.0	2.78	100	0.77
5.0	4.04	93.75	0.83
10.0	5.86	85.42	1.45
15.0	4.84	89.58	1.65

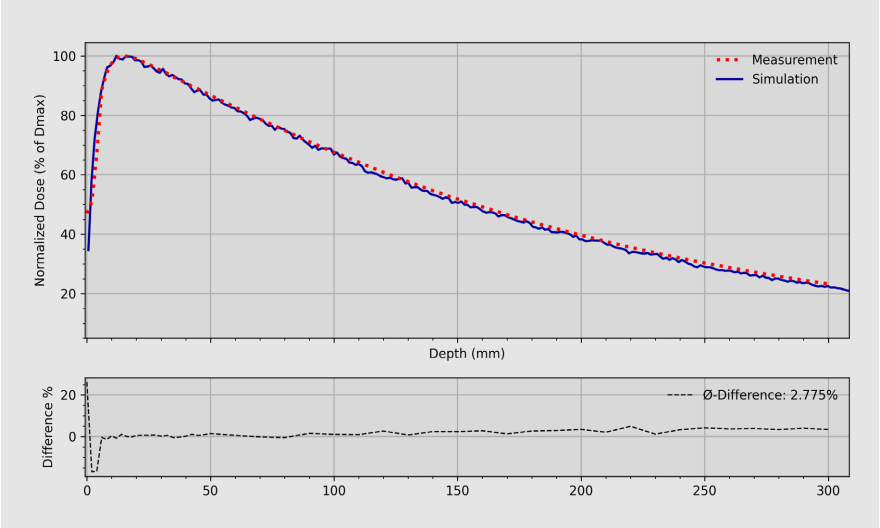

(a)

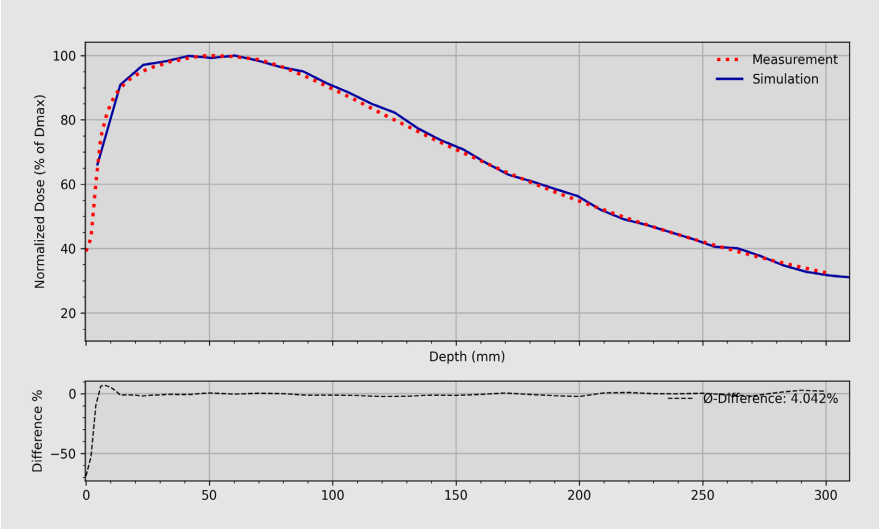

(b)

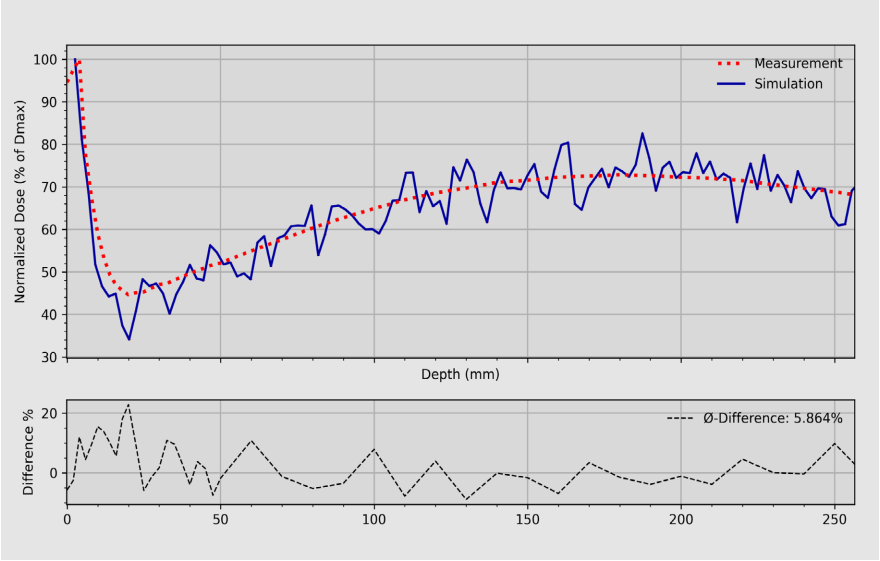

(c)

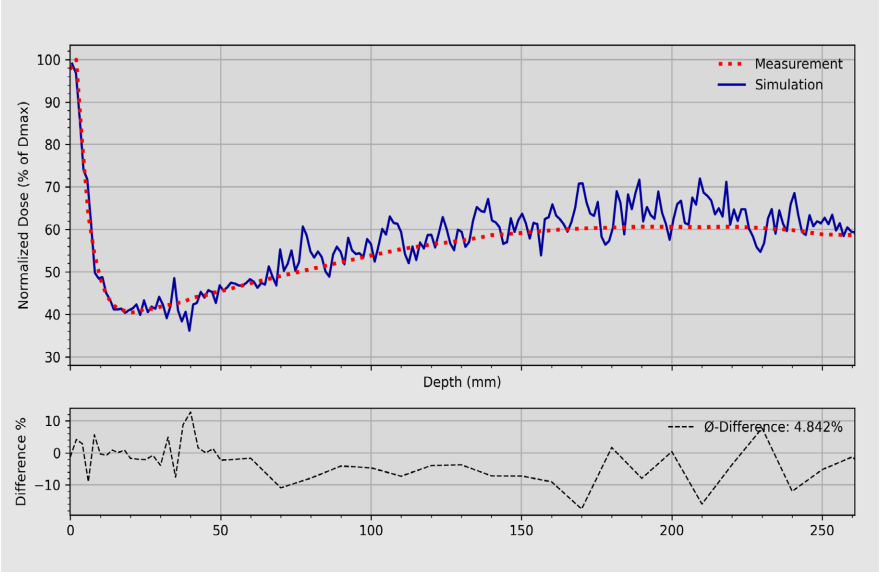

(d)

Figure 5. The PDDs curves from 6 MV beam for 10 cm ×10 cm field size on central axis (a), at 5 cm (b), 10 cm (c), and 15 cm (d) from central axis. The statistical uncertainty associated with the simulations were 0.77%, 0.83%, 1.45%, and 1.65% respectively. All curves are normalized to dose at Dmax.

Table 2 shows the relative difference and gamma passing rate between the measured and simulated dose profile for an energy of 6MV, along the in-plane direction for field sizes of 5 × 5 cm^2, 10 × 10 cm^2, 15 × 15 cm^2, and 20 × 20 cm^2 at depths of 1.5 cm, 5.0 cm and 10.0 cm in the water phantom for each field size. For curves obtained at a depth of 10 cm (**Figure 6**). The comparison between the measured and simulated curves shows a good agreement. The simulation uncertainties associated with each curve are equal to about 1%. **Table 2** and **Figure 6** are represented below respectively.

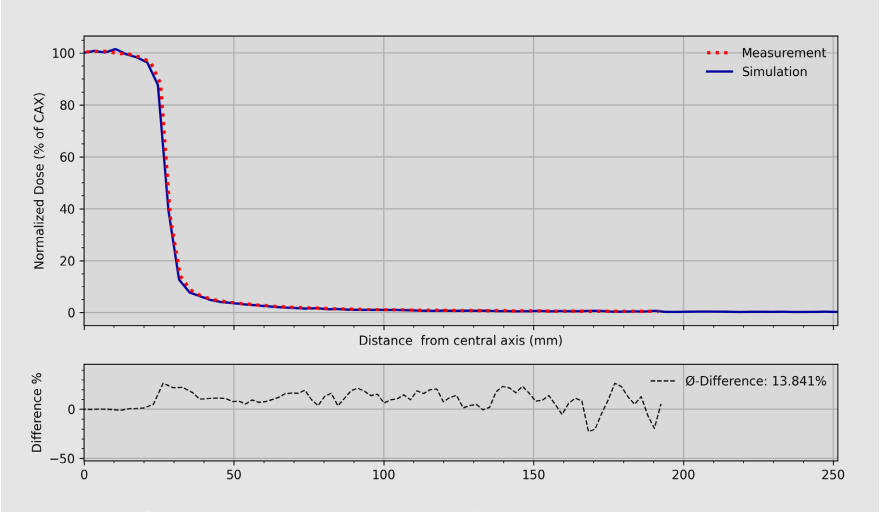
Measurement
Simulation
Normalized Dose (% of CAX)
Distance from central axis (mm)
Difference %
Ø-Difference: 13.841%

(a)

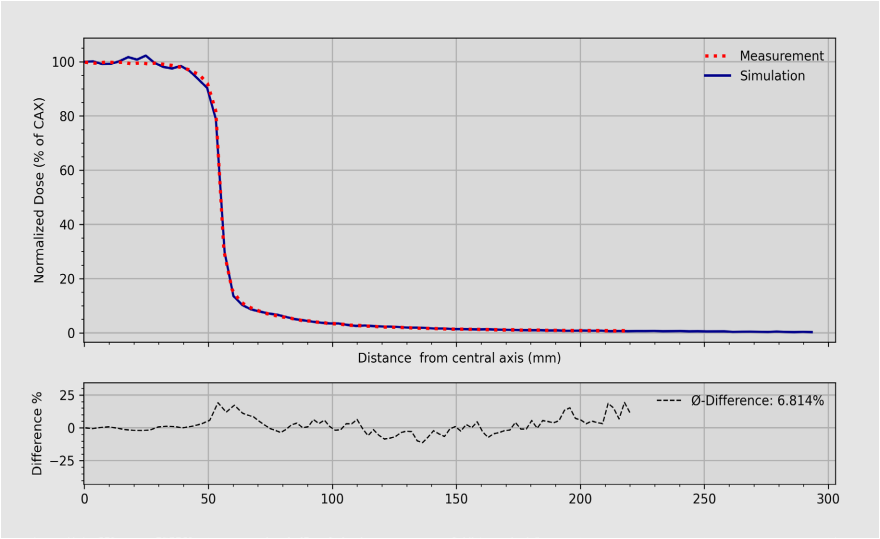
Measurement
Simulation
Normalized Dose (% of CAX)
Distance from central axis (mm)
Difference %
Ø-Difference: 6.814%

(b)

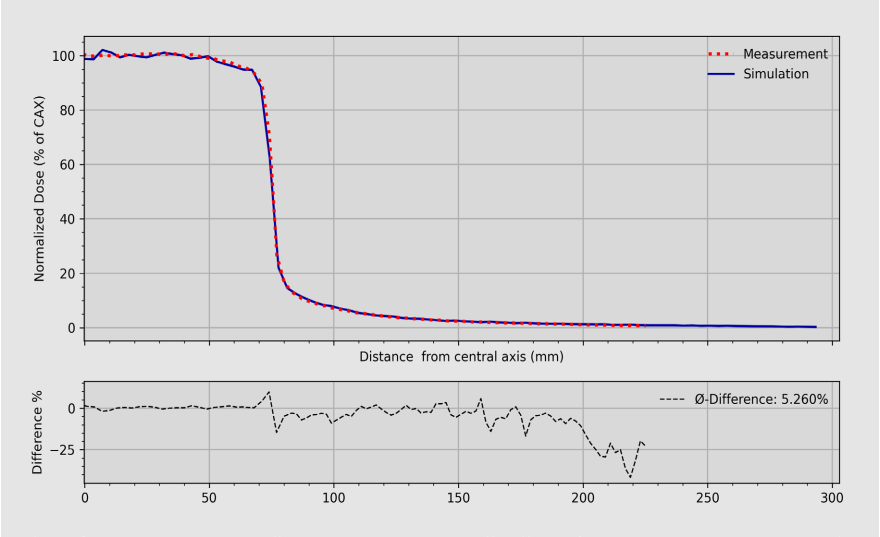
Measurement
Simulation
Normalized Dose (% of CAX)
Distance from central axis (mm)
Difference %
Ø-Difference: 5.260%

(c)

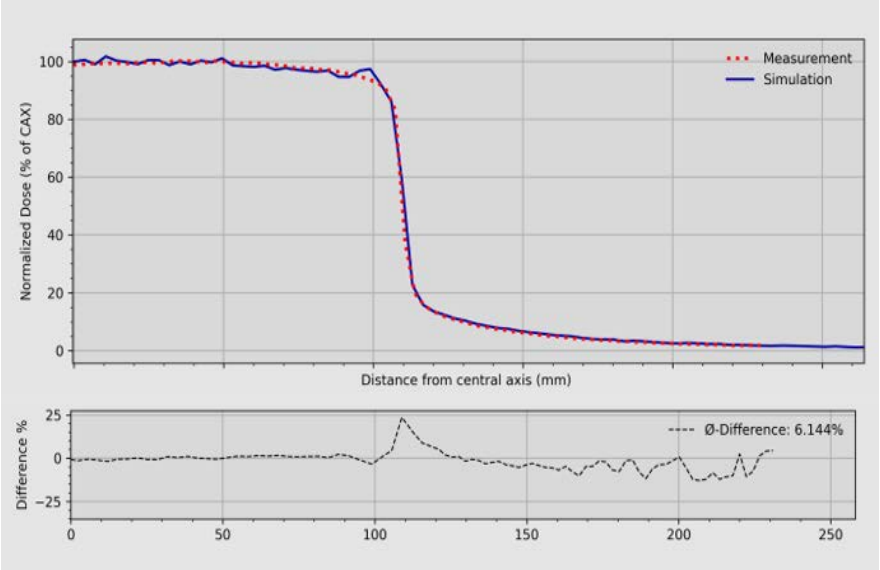

(d)

Figure 6. Lateral dose profiles for 5 cm × 5 cm (a), 10 cm × 10 cm (b), 15 cm × 15 cm (c), and 20 cm × 20 cm (d) fields at depth 10 cm. The statistical uncertainty associated with the simulations were 1.5%, 0.91%, 0.85%, and 0.82% respectively. All curves are normalized to dose of CAX.

Table 2. The relative difference and gamma index values between the measured and simulated off-field dose profiles for field sizes 5 × 5, 10 × 10, 15 × 15 and 20 × 20 cm^2 at 1.5, 5.0 and 10.0 cm for each dose profile, and statistical uncertainty of simulation.

Field size (cm^2)	Depth (cm)	Relative difference (%)	Gamma passing rate (%)	Uncertainty (%)
5 × 5	1.5	13.11	100.00	0.93
	5.0	14.78	99.40	0.97
	10	13.84	98.20	1.05
10 × 10	1.5	8.09	100.00	0.83
	5.0	9.35	99.45	0.85
	10	6.81	98.91	0.91
15 × 15	1.5	8.41	100.00	0.78
	5.0	8.43	94.47	0.81
	10	5.26	95.36	0.85
20 × 20	1.5	5.94	98.68	0.76
	5.0	8.88	97.02	0.77
	10	6.14	95.81	0.82

4. Discussion

The off-field and in-field dose measurement results for the 6 MV Elekta Synergy head model was in agreement with other studies that modelled the Elekta linear accelerator, by comparing particularly the measured PDDs and the dose profiles with simulated. In this context, Al-Saleh *et al.* [20] modelled a 6 MV Elekta linear accelerator for in-field and off-field dose measurement using the BEAMnrc/DOSX codes. Hence, the dose difference between measured and simulate was 15.0% [20]. Kry *et al.* [18] [21] modelled the off-field dosimetry from a Varian Clinac-X 2100 accelerator head, using the MCNPX Monte Carlo code for 6 MV and 18 MV photon energies. Off-field lateral dose profiles were measured with thermoluminescence dosimeters (Harshaw, TLD-100) in a rectangular phantom composed with acrylic blocks at SSD of 100 cm. They concluded that the difference between measurement and simulation dose ranged between 0.0% and 42.0%, with an average absolute difference of 23.0%, and simulated doses from their model agreed with measured data to an average absolute accuracy of 16% [18] [21]. The dose difference between measurements and simulations reported by Bednarz *et al.*, [16] on their off-field dose model using the Varian linear accelerator of a 6 MV was 14.0%. Sinousy *et al.* [22] simulated a 6 MV Siemens Primus Linac using the Geant4/GATE code. The latter obtained a gamma pass rate of 100.0% at 0.0 cm, 100.0% at 5.0 cm, and 76.70% at 7.5 cm from the beam axis [22]. Almberg *et al.* [23] reported that off-field PDD curves for half-beam blocked, a gamma pass rate was 96.70% at 8.5 cm from the central axis with a MC model developed using the BEAMnrc MC Code for the Elekta Synergy Linac.

Measurements and simulations of PDDs curves at 15.0 cm from the center axis were fixed as a limit because dose measurements in the water phantom could not be carried out over the full distance between the central axis and the phantom wall, due to the limited mechanical movement of the ionization chamber. This statement was also confirmed by the study of Sinousy *et al.* [22] and Kry *et al.* [21] showed that the accuracy in the bean-line component model for the off-field doses can be achieved up to 15.0 cm from the edge of the field, because beyond this distances, the accuracy becomes less reliable. The curves of measured and simulated PDDs at 0.0 cm, 5.0 cm, 10.0 cm and 15.0 cm respectively of central axis were compared. The results presented in **Figure 5(a)** and **Figure 5(b)**, show a good agreement between measurement and simulation with the gamma pass rates of 100.0% and 93.75%, and the differences of 2.78 % and 4.04% respectively (**Table 1**). The two curves almost had identical trends where the dose increased until a certain d_{max} and then decreased gradually. However, the PDDs at 10.0 cm and 15.0 cm of the central axis show different trends revealing an increase in the dose to the surface due to the contamination of electrons outside the field size. This dose decreases abruptly until 1.5 cm, then increases gradually due to the scattering of photons in water. The gamma pass rates was 85.42% and 89.58% for the PDDs at 10.0 cm and 15.0 cm of the central

axis respectively; and the average dose difference between the measured and simulated PDDs curves was 5.86% and 4.84% respectively. The statistical uncertainties in the simulated doses were less than 1.1% on the central axis and penumbra, and up to 1.65% at 15 cm from the central axis, which could explain the noisy observed, due to the lower fluence generated by scattered photons in the off-field zone. These values obtained in-field are the same order of magnitude as those obtained by Al-Saleh *et al.* [20] where the dose difference between the measured and simulated PDDs curves was less than 9.0%. As Sinousy *et al.* [22], the same trend of gamma pass rate (100.0%) in field was observed. However, for off-field PDD curves, our gamma pass rates are higher than those reported by Sinousy *et al.* [22] at 7.5 cm from the axis (76.70%). These differences observed are due to the code used in the above-mentioned studies, or the half-beam blocked field size that helps to avoid beam divergence as reported by Almberg *et al.* [23] in their study, leading to an off-field profile curve at a constant distance from the field edge.

We have included measured and simulated dose profile curves for field sizes of 5 × 5 cm^2, 10 × 10 cm^2, 15 × 15 cm^2, and 20 × 20 cm^2 at different depths of 1.5 cm, 5.0 cm and 10.0 cm in a water phantom for each field size. **Figure 6** shows a comparison of the measured and simulated off-field dose in which a good agreement was observed with an average gamma pass rate for all field sizes at different depths considered in this study was 98.11%. The 20 × 20 cm^2 field size showed the best agreement, with an average difference of 4.0% between measured and simulated values, and a maximum different of less than 15.0% at 5.0 cm depth. The best agreement was achieved for 10 × 10 cm^2 and 15 × 15 cm^2 fields, where the average difference between the measured and calculated dose was 8.05% and 7.4% respectively, and the maximum difference which was less than 9.53% and 8.43 at 5 cm depth respectively. An acceptable agreement was also seen for the 5 × 5 cm^2 field where the average difference between the measured and calculated dose was 13.91 % with a maximum different of 14.78% at 5 cm depth. The average difference between measurement and simulation for all considered field sizes at different depths was 9.10%. This value is below reported values by the previous studies mentioned [16] [18] [20] [21]. This difference could be due to the difference in the MC code and Linac used. For all considered field sizes and depths, the average statistical uncertainty was 0.86%. Statistical uncertainty increased with depth and decreased with field size (**Table 2**). This decrease of statistical uncertainty with increasing field size was due to higher photon fluence in the off-field region from larger field sizes.

In the present study, all beams used were open square fields size in the water phantom, in order to facilitate validation of the MC model for the 6 MV Elekta Synergy photon beam with a minimal configuration. The latter is an essential condition before any proposed future studies to confidently simulate off-field doses for real patients under real conditions. Actual treatment conditions may influence the out-of-field dose, and consequently the occurrence of radia-

tion-induced secondary cancer. In this context, Joosten *et al.* [24] showed that the off-field dose was higher for 3D-CRT compared to 2D-RT and IMRT. According to the observations of Diallo *et al.* [25], the majority of secondary cancers were located in the region of the beam boundary. Only 9 out of 115 cases of secondary cancer could occur at distances greater than 20 cm from the beam boundary.

5. Conclusion

This paper described the Monte Carlo model validation in order to simulate the off-field dose for a 6 MV Linac Elekta Synergy. The results obtained showed a good agreement between the measured and simulated dose. Subsequently, the tool used is able to simulate accurately the Linac dosimetry properties including key components of the gas pedal head that can be modelled more precisely according to the manufacturer's specifications. The TOPAS-MC model validated in this work can also be used for future studies for a validation in heterogeneous environments, followed by dose assessment in off-field organs for real clinical cases, and consequently estimate radiation-induced secondary cancer risks. To this end, patient CT images could be directly integrated into the TOPAS-MC model instead of using a geometric water phantom.

Conflicts of Interest

The authors declare no conflicts of interest regarding the publication of this paper.

References

[1] Preston, D.L., Shimizu, Y., Pierce, D.A., Suyama, A. and Mabuchi, K. (2003) Studies of Mortality of Atomic Bomb Survivors. Report 13: Solid Cancer and Noncancer Disease Mortality: 1950-1997. *Radiation Research*, **160**, 381-407. https://doi.org/10.1667/rr3049

[2] Wilde, G. and Sjostrand, J. (1997) A Clinical Study of Radiation Cataract Formation in Adult Life Following Gamma Irradiation of the Lens in Early Childhood. *British Journal of Ophthalmology*, **81**, 261-266. https://doi.org/10.1136/bjo.81.4.261

[3] D'Agostino, E., Bogaerts, R., Defraene, G., de Freitas Nascimento, L., Van den Heuvel, F., Verellen, D., *et al.* (2013) Peripheral Doses in Radiotherapy: A Comparison between IMRT, VMAT and Tomotherapy. *Radiation Measurements*, **57**, 62-67. https://doi.org/10.1016/j.radmeas.2013.04.016

[4] Xu, X.G., Bednarz, B. and Paganetti, H. (2008) A Review of Dosimetry Studies on External-Beam Radiation Treatment with Respect to Second Cancer Induction. *Physics in Medicine and Biology*, **53**, R193-R241. https://doi.org/10.1088/0031-9155/53/13/r01

[5] Stovall, M., Blackwell, C.R., Cundiff, J., Novack, D.H., Palta, J.R., Wagner, L.K., *et al.* (1995) Fetal Dose from Radiotherapy with Photon Beams: Report of AAPM Radiation Therapy Committee Task Group No. 36. *Medical Physics*, **22**, 63-82. https://doi.org/10.1118/1.597525

[6] Chetty, I.J., Curran, B., Cygler, J.E., DeMarco, J.J., Ezzell, G., Faddegon, B.A., *et al.*

(2007) Report of the AAPM Task Group No. 105: Issues Associated with Clinical Implementation of Monte Carlo-Based Photon and Electron External Beam Treatment Planning. *Medical Physics*, **34**, 4818-4853. https://doi.org/10.1118/1.2795842

[7] Low, D.A., Harms, W.B., Mutic, S. and Purdy, J.A. (1998) A Technique for the Quantitative Evaluation of Dose Distributions. *Medical Physics*, **25**, 656-661. https://doi.org/10.1118/1.598248

[8] Matsubara, H. (2023) Neutron Dose from a 6-MV X-Ray Beam in Radiotherapy. *Radiological Physics and Technology*, **16**, 186-194. https://doi.org/10.1007/s12194-023-00705-6

[9] Musolino, S.V. (2001) Absorbed Dose Determination in External Beam Radiotherapy: An International Code of Practice for Dosimetry Based on Standards of Absorbed Dose to Water; Technical Reports Series No. 398. *Health Physics*, **81**, 592-593. https://doi.org/10.1097/00004032-200111000-00017

[10] Perl, J., Shin, J., Schümann, J., Faddegon, B. and Paganetti, H. (2012) TOPAS: An Innovative Proton Monte Carlo Platform for Research and Clinical Applications. *Medical Physics*, **39**, 6818-6837. https://doi.org/10.1118/1.4758060

[11] Agostinelli, S., Allison, J., Amako, K., Apostolakis, J., Araujo, H., Arce, P., *et al.* (2003) GEANT4—A Simulation Toolkit. *Nuclear Instruments and Methods in Physics Research Section A*: *Accelerators*, *Spectrometers*, *Detectors and Associated Equipment*, **506**, 250-303. https://doi.org/10.1016/s0168-9002(03)01368-8

[12] Faddegon, B., Ramos-Méndez, J., Schuemann, J., McNamara, A., Shin, J., Perl, J., *et al.* (2020) The TOPAS Tool for Particle Simulation, a Monte Carlo Simulation Tool for Physics, Biology and Clinical Research. *Physica Medica*, **72**, 114-121. https://doi.org/10.1016/j.ejmp.2020.03.019

[13] Shin, J., Perl, J., Schümann, J., Paganetti, H. and Faddegon, B.A. (2012) A Modular Method to Handle Multiple Time-Dependent Quantities in Monte Carlo Simulations. *Physics in Medicine and Biology*, **57**, 3295-3308. https://doi.org/10.1088/0031-9155/57/11/3295

[14] TOPAS Tool for Particle Simulation. https://www.topasmc.org/

[15] Seco, J. and Verhaegen, F. (2013) Monte Carlo Techniques in Radiation Therapy. CRC Press.

[16] Bednarz, B. and Xu, X.G. (2009) Monte Carlo Modeling of a 6 and 18 MV Varian Clinac Medical Accelerator for in-Field and Out-of-Field Dose Calculations: Development and Validation. *Physics in Medicine and Biology*, **54**, N43-N57. https://doi.org/10.1088/0031-9155/54/4/n01

[17] Brun, R. and Rademakers, F. (1997) ROOT—An Object Oriented Data Analysis Framework. *Nuclear Instruments and Methods in Physics Research Section A*: *Accelerators*, *Spectrometers*, *Detectors and Associated Equipment*, **389**, 81-86. https://doi.org/10.1016/s0168-9002(97)00048-x

[18] Kry, S.F., Titt, U., Followill, D., Pönisch, F., Vassiliev, O.N., White, R.A., *et al.* (2007) A Monte Carlo Model for Out-of-Field Dose Calculation from High-Energy Photon Therapy. *Medical Physics*, **34**, 3489-3499. https://doi.org/10.1118/1.2756940

[19] Walters, B.R.B., Kawrakow, I. and Rogers, D.W.O. (2002) History by History Statistical Estimators in the Beam Code System. *Medical Physics*, **29**, 2745-2752. https://doi.org/10.1118/1.1517611

[20] Al-Saleh, W.M. and Hugtenburg, R.P. (2023) Monte Carlo Modelling of a 6 MV Elekta Linear Accelerator for in-Field and Out-of-Field Dosimetry. *Radiation Physics and Chemistry*, **203**, Article 110584. https://doi.org/10.1016/j.radphyschem.2022.110584

[21] Kry, S.F., Titt, U., Pönisch, F., Followill, D., Vassiliev, O.N., Allen White, R., *et al.* (2006) A Monte Carlo Model for Calculating Out-of-Field Dose from a Varian Beam. *Medical Physics*, **33**, 4405-4413. https://doi.org/10.1118/1.2360013

[22] Mohamed Sinousy, S.D., Marouf Attalla, A.E., Hassan Fathy, I., Fathi Ahmed, E.F. and Ahmed Farouk, E. (2020) Validation of Monte Carlo Model for Dose Evaluation Outside the Treatment Field for Siemens 6MV Beam. *Iranian Journal of Medical Physics*, **17**, 410-420. https://doi.org/10.22038/IJMP.2019.42881.1646

[23] Almberg, S.S., Frengen, J. and Lindmo, T. (2012) Monte Carlo Study of In-Field and Out-of-Field Dose Distributions from a Linear Accelerator Operating with and without a Flattening-Filter. *Medical Physics*, **39**, 5194-5203. https://doi.org/10.1118/1.4738963

[24] Joosten, A., Matzinger, O., Jeanneret-Sozzi, W., Bochud, F. and Moeckli, R. (2013) Evaluation of Organ-Specific Peripheral Doses after 2-Dimensional, 3-Dimensional and Hybrid Intensity Modulated Radiation Therapy for Breast Cancer Based on Monte Carlo and Convolution/Superposition Algorithms: Implications for Secondary Cancer Risk Assessment. *Radiotherapy and Oncology*, **106**, 33-41. https://doi.org/10.1016/j.radonc.2012.11.012

[25] Diallo, I., Haddy, N., Adjadj, E., Samand, A., Quiniou, E., Chavaudra, J., *et al.* (2009) Frequency Distribution of Second Solid Cancer Locations in Relation to the Irradiated Volume among 115 Patients Treated for Childhood Cancer. *International Journal of Radiation Oncology Biology Physics*, **74**, 876-883. https://doi.org/10.1016/j.ijrobp.2009.01.040